ACTA ET COMMENTATIONES UNIVERSITATIS TARTUENSIS DE MATHEMATICA
Volume 29, Number 1, June 2025
Available online at https://ojs.utlib.ee/index.php/ACUTM

Analysis of elastic conical shells of variable thickness with rib-reinforcement

Jaan Lellep and Ella Puman

Abstract. Circular conical shells of an elastic material subjected to the static distributed lateral pressure are studied under the assumption of axial symmetry. The shell with variable thickness is strengthened with the help of circular ribs. Necessary optimality conditions are derived using theory of optimal control. The case of the shell with a singular circular rib is treated in greater detail. The optimal position of the stiffener is established when the cost function coincides with the mean deflection of the shell.

1. Introduction

Thin-walled plates and shells are widely used in technology and mechanical engineering. The dynamic plastic response of axisymmetric plates was initially studied by Hopkins and Prager [4] in the case of an ideal rigid-plastic material. Later the solution by Hopkins and Prager was extended to axisymmetric shells and various types of dynamic loading by Florence [2], Jones [5], Niepostyn and Stanczyk [11], Wang et al. [15].

The conical shells have deserved much less heed in the literature. Stawiarski et al. [14] investigated the global buckling behavior of the conical shells with the variable fiber orientation and thickness.

However, the plastic dynamic response of conical shells to impulsive loading and blast loading was studied by Lellep and Puman [8], [9], [10]. It was assumed in [10] that the material of shells under investigation obeys the Johansens yield condition and the associated flow law. Several authors, including Ross [12], also Lellep and Puman [9], [10], have studied the stress-strain state of elastic conical shells with ring stiffeners.

Received April 16, 2024.
2020 *Mathematics Subject Classification.* 74C05.
Key words and phrases. Elasticity, rib-reinforced conical shell, thin walled shell, variable thickness.
https://doi.org/10.12697/ACUTM.2025.29.01
Corresponding author: Ella Puman

In the present paper, the circular conical shell strengthened with ring stiffeners will be treated as a conical shell with piece-wise constant shell wall thickness. The main concern will be the determination of optimal locations of stiffeners analytically and numerically.

2. Formulation of the problem

Consider an axisymmetric conical shell with the radii a and R of the bottoms. Figure 1 depicts a two-dimensional model derived from a planar section of a real structure. The central boss with radius a is assumed to be a perfectly rigid part of the structure. The shell is subjected to uniformly distributed lateral loading of intensity P. Let the thickness of the shell wall be h and the thickness of ribs h_1. The stiffeners are located at $r_i \in (a_i, b_i)$, $i = 1, \ldots, n$. In the present paper, the attention is focused on the case when both the inner edge at $r = a_0$ and the outer edge at $r = R$ are simply supported or pinned edges. This means that the boundary conditions are

$$M_1(a) = 0, N_1(a) = 0 \tag{1}$$

and

$$M_1(R) = 0. \tag{2}$$

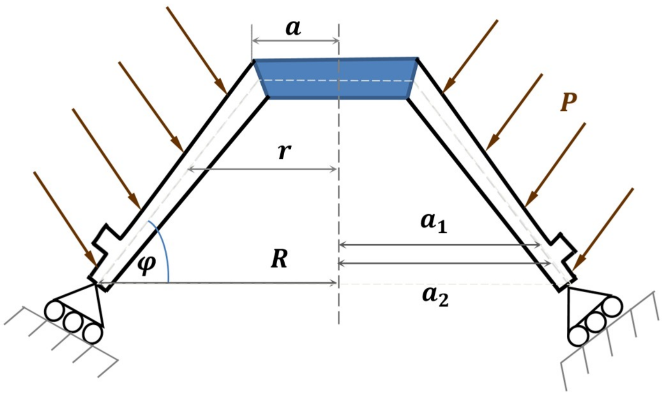

FIGURE 1. Ring-stiffened conical shell.

In (1) and (2), M_1 stands for the radial bending moment and N_1 is the radial membrane force. In what follows, M_2 and N_2 denote the circumferential bending moment and the membrane force, respectively. The displacements in the radial and circumferential directions are denoted by W and U, respectively. According to the current boundary conditions, one has

$$W(a) = 0, W(R) = 0, W'(a) = 0. \tag{3}$$

The aim of the study is to determine the stress-strain state of the shell and to define the optimal locations of stiffeners (in the case of an optimization problem) so that the mean deflection is minimal. The area between the deflection graph and the r-axis reaches a minimum value for the same volume of material compared to a cone of constant thickness.

3. Governing equations

Let $\varepsilon_1, \varepsilon_2$ stand for the linear extension ratios and κ_1, κ_2 for the curvatures of the conical shell element in the radial and circumferential directions, respectively. The strains can be calculated as (see Ventsel and Krauthammer [16])

$$\begin{aligned} \varepsilon_1 &= \frac{dU}{dr}\cos\varphi, \\ \varepsilon_2 &= \frac{1}{r}\left(U\cos\varphi + W\sin\varphi\right), \\ \kappa_1 &= -\frac{d^2W}{dr^2}\cos^2\varphi, \\ \kappa_2 &= -\frac{1}{r}\frac{dW}{dr}\cos^2\varphi, \end{aligned} \tag{4}$$

where φ denotes the angle of inclination of the middle surface of the truncated cone. Hooke's law furnishes the linear relations between strains (see [16]) and stresses

$$\begin{aligned} N_1 &= B_j(\varepsilon_1 + \nu\varepsilon_2), \\ N_2 &= B_j(\varepsilon_2 + \nu\varepsilon_1), \\ M_1 &= D_j(\kappa_1 + \nu\kappa_2), \\ M_2 &= D_j(\kappa_2 + \nu\kappa_1) \end{aligned} \tag{5}$$

for each region (a_j, a_{j+1}). In (5) ν stands for the Poisson ratio and

$$B_j = \frac{2Eh_j}{1-\nu^2}, D_j = \frac{Eh_j^3}{12(1-\nu^2)}, \tag{6}$$

where E is the Young modulus of the material. The equilibrium equations of axisymmetric conical shells can be presented as (see Kaliszky [5], Chakrabarty [1], Soedel [13])

$$\begin{aligned} &\frac{d}{dr}(rN_1) - N_2 = 0, \\ &\frac{d}{dr}\left(\frac{d}{dr}(rM_1) - M_2\right) + N_2\frac{\sin\varphi}{\cos^2\varphi} + \frac{1}{\cos^2\varphi}Pr = 0. \end{aligned} \tag{7}$$

It is reasonable to introduce the state variables

$$y_1 = W,\ y_2 = Z,\ y_3 = U,\ y_4 = N_1,\ y_5 = M_1. \tag{8}$$

4. Necessary optimality conditions

The problem of determination of optimal positions for stiffeners will be considered as a problem of optimal control. Let the cost function be

$$J = \int_a^R y_1 r \, dr. \tag{9}$$

The state equations can be presented according to (7)–(8) as

$$\begin{aligned}
y_1' &= y_2, \\
y_2' &= -\frac{y_5}{D\cos^2\varphi} - \frac{\nu}{r} y_2, \\
y_3' &= \frac{y_4}{D\cos^2\varphi} - \frac{\nu}{r}(y_3 + y_1 \tan\varphi), \\
y_4' &= \frac{1}{r}(N_2 - y_4), \\
y_5' &= \frac{1}{r}(M_2 - y_5) - y_4 \frac{\sin\varphi}{\cos^2\varphi} - \frac{P(r^2 - a^2)}{2r\cos^2\varphi},
\end{aligned} \tag{10}$$

where primes denote the differentiation with respect to r. Note that the variables N_2, M_2 will be handled as auxiliary variables and

$$B = \frac{Eh}{1-\nu^2}, \; D = \frac{Eh^3}{12(1-\nu^2)}. \tag{11}$$

To derive the optimality conditions, let us consider the extended functional

$$\begin{aligned}
J_* = \sum_{i=0}^{n} \int_{a_i}^{b_i} \Big\{ & y_1 r + \psi_1(y_1' - y_2) + \psi_2 \left(y_2' + \frac{y_5}{D\cos^2\varphi} + \frac{\nu}{r} y_2 \right) \\
& + \psi_3 \left(y_3' - \frac{y_4}{D\cos^2\varphi} + \frac{\nu}{r}(y_3 + y_1\tan\varphi) \right) \\
& + \psi_4 \left(y_4' - \frac{1}{r}(N_2 - y_4) \right) \\
& + \psi_5 \left(y_5' - \frac{1}{r}(M_2 - y_5) + y_4 \frac{\sin\varphi}{\cos^2\varphi} + \frac{P(r^2 - a^2)}{2r\cos^2\varphi} \right) \\
& + \varphi_1 \Phi_1 + \varphi_2 \Phi_2 \Big\} \, dr,
\end{aligned} \tag{12}$$

where $b_i = a_{i+1}$ for $i = 0, \ldots, n; a_0 = a, b_n = a_{n+1} = R$. In (10) and (12) the auxiliary variables are

$$
\begin{aligned}
\Phi_1 &= B\left(y_3' \cos\varphi + \frac{\nu}{r}\left(y_3 \cos\varphi + y_1 \sin\varphi\right)\right) - y_4,\\
N_2 &= \nu y_4 + \frac{B}{r}(1-\nu^2)(y_3\cos\varphi + y_1 \sin\varphi),\\
M_2 &= \nu y_5 + \frac{D}{r}(1-\nu^2)\, y_2 \cos^2\varphi,\\
\Phi_2 &= -D\left(y_2' + \frac{\nu}{r} y_2\right)\cos^2\varphi - y_5,
\end{aligned}
\tag{13}
$$

for $r \in (a_i, a_{i+1})$; $i = 0, \ldots, n$. Calculating the total variation of J_* and equalizing it to zero leads to the set of equations

$$
H(a_i + 0) - H(a_i - 0);\ i = 1, \ldots, n, \tag{14}
$$

where H is the Hamiltonian function. In (12) ψ_j stands for the adjoint variable to be calculated as

$$
\psi_j' = -\frac{\partial H}{\partial y_j} \tag{15}
$$

for each $j = 1, \ldots, 5$. The Hamiltonian function is defined as

$$
\begin{aligned}
H = &- y_1 r + \psi_1 y_2 + \psi_2\left(-\frac{y_5}{D\cos^2\varphi} - \frac{\nu}{r} y_2\right)\\
&+ \psi_3\left(\frac{y_4}{D\cos^2\varphi} - \frac{\nu}{r}(y_3 + y_1 \tan\varphi)\right) + \frac{\psi_4}{r}\left(N_2 - y_4\right)\\
&+ \psi_5\left(\frac{1}{r}(M_2 - y_5) - y_4\frac{\sin\varphi}{\cos^2\varphi} - \frac{P(r^2 - a^2)}{2r\cos^2\varphi}\right)\\
&+ \varphi_1\Phi_1 + \varphi_2\Phi_2,
\end{aligned}
\tag{16}
$$

where φ_1, φ_2 stand for the slack variables, and Φ_1, Φ_2 are defined by (13). According to (15) and (16), the adjoint system can be presented as

$$
\begin{aligned}
\psi_1' &= r + \frac{\psi_3 \nu \tan\varphi}{r} - \frac{\psi_4}{r}\frac{\partial N_2}{\partial y_1} - \varphi_1 \frac{\partial \Phi_1}{\partial y_1},\\
\psi_2' &= -\psi_1 + \frac{\nu}{r}\psi_2 - \frac{\psi_5}{r}\frac{\partial M_2}{\partial y_2} - \varphi_2\frac{\partial \Phi_2}{\partial y_2},\\
\psi_3' &= \psi_3\frac{\nu}{r} - \frac{\psi_4}{r}\frac{\partial N_2}{\partial y_3} - \varphi_1\frac{\partial \Phi_1}{\partial y_3},\\
\psi_4' &= -\frac{\psi_3}{D\cos^2\varphi} + \psi_5\frac{\sin\varphi}{\cos^2\varphi} - \frac{\psi_4}{r}(\nu - 1) + \varphi_1,\\
\psi_5' &= \frac{\psi_5}{r}(1-\nu) + \frac{\psi_2}{D\cos^2\varphi} + \varphi_2.
\end{aligned}
\tag{17}
$$

The transversality conditions for the current problem are

$$\psi_2(a) = 0,\ \psi_4(a) = 0,\ \psi_5(a) = 0,\ \psi_2(R) = 0,\ \psi_4(R) = 0. \tag{18}$$

The systems (10) and (17) should be solved together, making use of (13) and suitable boundary conditions (1)–(3), (18).

5. Numerical results and discussion

Numerical results are obtained for conical frusta with variable thickness $h(r)$ and the case of a unique rib placed at $r = a_1$ to the shell wall with variable thickness. Calculations are carried out for the shell with

$$R = 1\,\mathrm{m},\ a = 0.1 - 0.7\,\mathrm{m}, \varphi = 17^\circ,\ p = 50\,\mathrm{GPa}.$$

Material constants are

$$E = 210\,\mathrm{GPa},\ \nu = 0.3.$$

The thickness of the rib is $h_1 = 0.05\,\mathrm{m}$. The results of calculations are presented in Tables 1 and 2, and Figures 2–6. The results for the cases

$$h(r) = ce^{-\frac{r^2}{2}}, e = \frac{S_{opt}}{S_*}, c = \frac{1}{25}, \tag{19}$$

$$h_* = \frac{2c}{R^2 - a^2}\left(e^{-\frac{a^2}{2}} - e^{-\frac{R^2}{2}}\right) \tag{20}$$

are accommodated in Table 1. In Table 2, the thickness of the reference shell is calculated,

$$h_* = \frac{2c}{R^2 - a^2}\left(e^{-\frac{a^2}{2}} - e^{-\frac{R^2}{2}} + e^{-\frac{a_2^2}{2}} - e^{-\frac{a_1^2}{2}}\right) + \frac{h_1}{R^2 - a^2}(a_2^2 - a_1^2). \tag{21}$$

Here, the material volume of the shell with variable thickness is equal to that of the shell with constant thickness $V_{opt} = V_{h_*}$, where h_* denotes the constant thickness of the reference shell, V_{opt} is the optimal material volume and S_{opt} is the optimal cost function value. The values of the coefficient of effectivity e are presented in the last column of Tables 1 and 2.

The distributions of transverse deflections are presented in the cases of shells with constant thickness and variable thickness for shells with a single stiffener. The stiffener is assumed to be located between $r = a_1$ and $r = a_2$, where $a_2 = a_1 + 0.015$. The width of the rib is assumed to be 1.5 cm.

In Figure 2, the solid curve corresponds to the shell with variable thickness $h(r) = \frac{1}{25}e^{-\frac{r^2}{2}}$ and the dashed line to the case of the reference shell with the same material volume, the shell wall thickness being $h_* = 0.03139\,\mathrm{m}$.

In Figures 3 and 4 solid lines correspond to the shells with stiffener at the optimal location between $r \in [a_1, a_2]$, and the dashed line is associated with the reference shell with the same material volume; the shell wall thickness is constant.

a	$h(a)$	h_*	S_{opt}	S_*	e
0.1	0.03980	0.031392	0.000057660	0.000082670	0.69724
0.2	0.03921	0.031139	0.000050823	0.000070197	0.72401
0.3	0.03824	0.030722	0.000040246	0.000053090	0.75808
0.4	0.03693	0.030151	0.000027199	0.000034084	0.79801
0.5	0.03530	0.029436	0.000015042	0.000017942	0.83837
0.6	0.03341	0.028592	0.000006485	0.000007417	0.87439
0.7	0.03131	0.027635	0.000001984	0.000002192	0.90492

TABLE 1. Shell with variable thickness.

In Figure 3 $a_1 = 0.71199\,\mathrm{m}, a_2 = 0.72699\,\mathrm{m}, h_* = 0.031809\,\mathrm{m}$, in Figure 4 $a_1 = 0.889034\,\mathrm{m}, a_2 = 0.904034\,\mathrm{m}, h_* = 0.028861\,\mathrm{m}$, respectively. From Figures 3 and 4, we see that the larger the inner radius, the larger the transverse deflections. Therefore, the economy of the optimal solution becomes smaller in the case of a bigger inner radius.

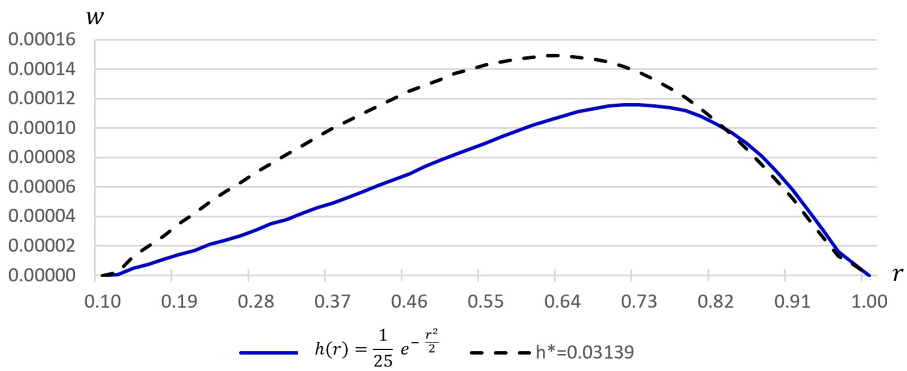

FIGURE 2. Transverse deflections (in meters) for $a = 0.1\,\mathrm{m}$.

Figure 5 depicts the comparison of transverse deflections for a shell with variable thickness, and the shell with a single stiffener was depicted in the case of $a = 0.1\,\mathrm{m}$. From Figure 5, we see that using the stiffener helps to reduce deflection.

Figure 6 depicts the displacements in the radial direction for the shell with variable thickness and with a single stiffener and for the reference shell with constant thickness and the same material volume in the case of $a = 0.1\,\mathrm{m}$. From Figure 6, we see that using the stiffener helps to reduce displacement.

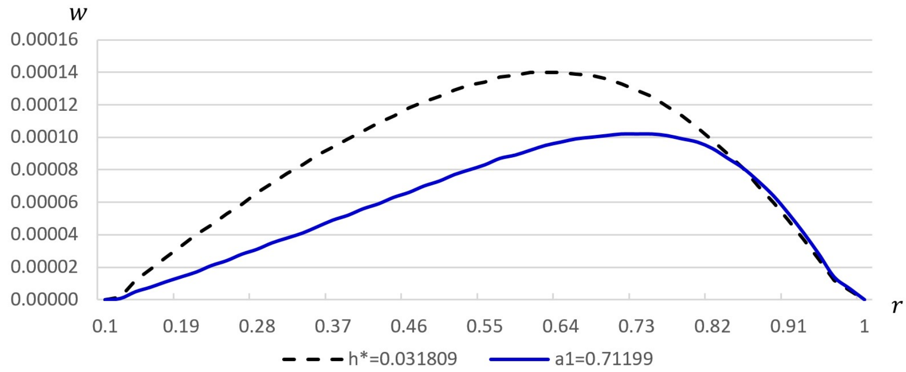

FIGURE 3. Transverse deflections (in meters) for the shell with single stiffener.

a	$h(a)$	a_1	h_*	S_{opt}	S_*	e
0.1	0.03980	0.71199	0.031809	0.000053063	0.000077701	0.682914
0.2	0.03921	0.71200	0.031569	0.000046274	0.000065628	0.705096
0.3	0.03824	0.71999	0.031185	0.000003485	0.000049109	0.709624
0.4	0.03693	0.77146	0.030720	0.000023545	0.000030742	0.765896
0.5	0.03523	0.81903	0.030149	0.000013037	0.000015631	0.834046
0.6	0.03341	0.84234	0.029474	0.000005583	0.000006199	0.900566
0.7	0.03130	0.88903	0.028861	0.000001606	0.000001692	0.949409

TABLE 2. Optimal locations for the stiffener.

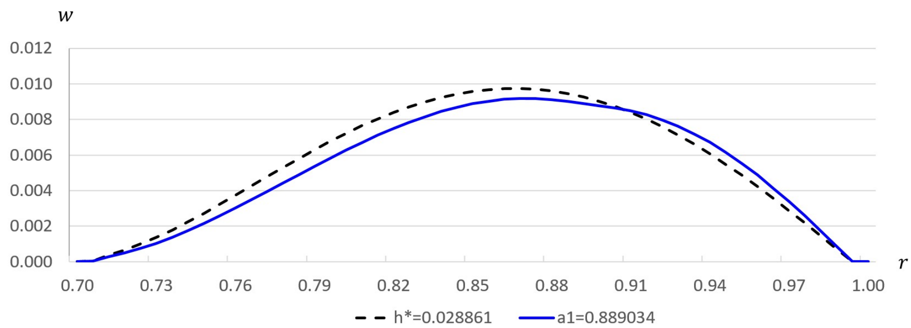

FIGURE 4. Transverse deflections (in meters) for the shell with a single stiffener for $a = 0.7\,\text{m}$.

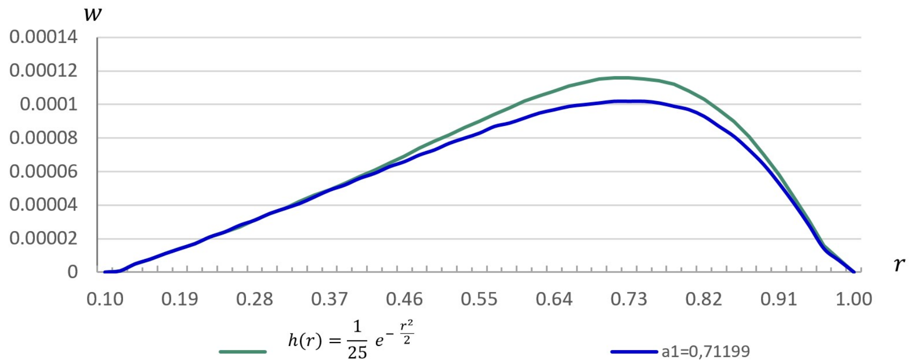

FIGURE 5. Transverse deflections (in meters) for the shell with variable thickness and the shell with single stiffener.

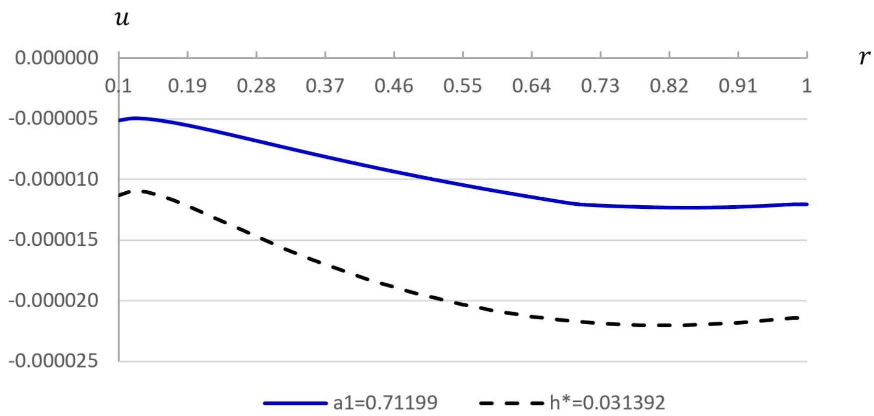

FIGURE 6. The displacements (in meters) in the radial direction for the shell with constant thickness and for the shell with variable thickness and with single stiffener.

6. Concluding remarks

A numerical analysis of axisymmetric conical shells subjected to the distributed lateral loading has been undertaken. The shell wall is with variable thickness. The conditions of optimality of ring stiffeners are derived analytically. Numerical results are obtained for the shell with variable thickness and when the shell is strengthened with a unique ring reinforcement.

Numerical analysis showed that a smaller inner radius results in a longer shell with lower transverse deflections. In contrast, a larger inner radius leads to larger transverse deflections, with the mean deflection remaining similar to that of a shell with constant thickness.

For the shell with constant thickness and comparing the results with the shell with variable thickness, we get 30 percent lower mean deflection when the inner radius is 10 centimeters and 10 percent if the inner radius is 70 centimeters, respectively (Table 1). For the shell with a single stiffener, we can get over 31.7 percent lower main deflection (for $a = 10\,\mathrm{cm}$) compared with the reference shell, which has a constant thickness and the same material volume (Table 2).

Acknowledgements

The authors thank the anonymous referees for very thorough and insightful reviews.

References

[1] J. Chakrabarty, *Applied Plasticity*, Springer, Berlin, 2000.
[2] A. L. Florence, *Clamped circular rigid-plastic plates under blast loading*, J. Appl. Mech. **33** (1966), 256–260.
[3] P. G. Hodge, *Limit Analysis of Rotationally Symmetric Shells*, Prentice Hall, New Jersey, 1963.
[4] H. G. Hopkins and W. Prager, *The load carrying capacities of circular plates*, J. Mech. Phys. Solids **2** (1953), 1–13.
[5] N. Jones, *Structural Impact*, CUP: Cambridge, 2012.
[6] S. Kaliszky, *Plasticity. Theory and Engineering Applications*, Elsevier, Amsterdam, 1989.
[7] R. W. Kuech and S. L. Lee, *Limit analysis of simply supported conical shells subjected to uniform internal pressure*, J. Franklin Inst. **280** (1965), 71–87.
[8] J. Lellep and E. Puman, *Optimization of inelastic conical shells with cracks*, Struct. Multidiscip. Optim. **33** (2007), 189–197.
[9] J. Lellep and E. Puman, *Optimal design of conical with stiffeners*. In: Proc. 3rd Int. Conf. of Optim. Anal. of Struct. OAS2015 (2015), 80–85. URL
[10] J. Lellep and E. Puman, *Plastic response of conical shells with stiffeners to blast loading*, Acta Comment. Univ. Tartu. Math. **24** (2020), 5–18. DOI
[11] D. Niepostyn and A. Stanczyk, *Pulse load of annular plastic plates supported on both edges*, Archiwum Mechaniki Stosowanej **33** (1981), 675–689. URL
[12] C. T. F. Ross, *Pressure Vessels under External Pressure: Statics and Dynamics*, Elsevier, London, 1990.
[13] W. Soedel, *Vibration of Shells and Plates*, Marcel Dekker, New York, 2004.
[14] A. Stawiarski, M. Chwał, M. Barski, and A. Muc, *The influence of the manufacturing constraints on the optimal design of laminated conical shells*, Compos. Struct. **235** (2020), 111820. DOI
[15] Y. Wang, M. Yu, Y. Xiao, and L. Li, *Dynamic plastic response of a circular plate based on unified strength theory*, Int. J. Impact Eng. **31** (2005), 25–40.
[16] E. Ventsel and T. Krauthammer, *Thin Plates and Shells. Theory, Analysis and Applications*, Marcel Dekker, New York, 2001.

Institute of Mathematics and Statistics, University of Tartu, 18 Narva str., 51009 Tartu, Estonia
E-mail address: jaan.lellep@ut.ee
E-mail address: ella.puman@ut.ee